AMERICAN ACADEMY OF OPHTHALMOLOGY®

Risk Analysis of Retinal Hemangioblastomas in Nonadvanced Stages of von Hippel–Lindau Syndrome Using Ultra-widefield Imaging: The ULTRA von Hippel–Lindau Study

Sebastiano Del Fabbro, MD,[1,2] Maria Vittoria Cicinelli, MD,[1,2] Rosangela Lattanzio, MD,[1,2] Soufiane Bousyf, MD,[1,2] Lorenza Bruno, MD,[1,2] Alessio Antropoli, MD,[1,2] Lorenzo Bianco, MD,[1,2] Elena Bruschi, MD,[1,2] Alessandro Arrigo, MD,[1,2] Giovanni Pipitone, MD,[1,5] Francesco Cei, MD,[1,3,4] Lucia Salerno, MD,[1,3,4] Alessandro Larcher, MD,[1,3,4] Andrea Salonia, MD,[1,3,4] Francesco Bandello, MD,[1,2] Maurizio Battaglia Parodi, MD,[1,2] on behalf of the OSR VHL Program

Purpose: To investigate the longitudinal progression, risk factors, and complications associated with retinal hemangioblastomas (RHs) in nonadvanced stages of von Hippel–Lindau (VHL) syndrome using ultra-widefield (UWF) imaging.

Design: Single-center longitudinal cohort study.

Subjects: Caucasian patients with genetically confirmed VHL syndrome.

Methods: Annual evaluations included dilated fundus examinations, UWF pseudocolor fundus retinal images, UWF fluorescein angiography, and OCT. Genetic analysis classified VHL mutations. Baseline RH counts and anatomical distributions were recorded as central (juxtapapillary, macular), peripheral, or both. Longitudinal follow-up tracked new RH formation and visual acuity (VA) values.

Main Outcome Measures: Cumulative incidence, incidence rate ratios (IRRs), and risk factors of new RHs assessed using mixed-effects negative binomial regression models. Hazard of recurrent RHs evaluated through Cox frailty models and longitudinal changes in VA.

Results: Among 78 eyes of 43 patients (mean age: 47.8 ± 13.6 years), 110 RHs were documented at baseline, with 3 (3%) centrally located, 35 (32%) peripherally, and 72 (65%) spanning both zones. von Hippel–Lindau variants were investigated in 37 patients: 19 had missense variants (51%), and 18 had presumed null alleles (49%), including nonsense (10 of 37; 27%), frameshift (1 of 37; 3%), splice site (1 of 37; 3%), and exon deletion mutations (6 of 37; 16%). Over a median follow-up of 31 months (interquartile range: 27–109), 35 (43%) eyes developed new RHs, with an incidence rate of 0.22 RHs per eye-year (95% confidence interval: 0.17–0.27). By the last available examination, 26 eyes (34%) remained disease-free, whereas17 (23%) showed no progression of existing RHs. Age reduced the IRR of new RHs by 4.2% annually ($P = 0.003$), whereas higher baseline tumor burden and vascular leakage increased the IRR significantly ($P < 0.001$ and $P = 0.03$, respectively). Peripheral RHs were the strongest predictor of recurrence (hazard ratio = 16.4, $P < 0.001$), whereas older age remained protective (hazard ratio = 0.96, $P = 0.04$). Visual acuity (logarithm of the minimum angle of resolution) worsened from 0.05 ± 0.2 (Snellen equivalent: 20/22) at baseline to 0.11 ± 0.3 (Snellen equivalent: 20/25) at the final visit.

Conclusions: Peripheral RHs and vascular leakage are significant risk factors for RH progression and recurrence in VHL syndrome. Although older age provides a protective effect, close monitoring of high-risk eyes is essential to enable timely intervention and preserve vision.

Financial Disclosure(s): Proprietary or commercial disclosure may be found in the Footnotes and Disclosures at the end of this article. *Ophthalmology Science 2025;5:100846*

von Hippel–Lindau (VHL) syndrome (Online Mendelian Inheritance in Man 608537) is a rare autosomal dominant disorder with an estimated incidence of 1 in 36 000 live births.[1] Affected individuals are at increased risk for a range of benign and malignant tumors, driven by mutations in the *VHL* gene on chromosome 3 that dysregulate hypoxia-inducible factor.[2,3] The hallmark manifestations of VHL syndrome include CNS hemangioblastomas, renal cell carcinomas, pancreatic neoplasms, pheochromocytomas, and retinal hemangioblastomas (RHs).[4]

Retinal hemangioblastomas are the initial manifestation of VHL syndrome in approximately 40% of patients and require lifelong monitoring due to their high recurrence

https://doi.org/10.1016/j.xops.2025.100846
ISSN 2666-9145/25

potential.[5] These tumors present bilaterally in 50% of cases and exhibit multifocality in one-third of affected eyes.[6] Risk factors such as younger age at onset, involvement of the contralateral eye, and type of genetic variant have been associated with a higher likelihood of multiple retinal tumors.[7] Despite their clinical significance, longitudinal studies evaluating the progression and characteristics of RHs remain limited.

The advent of ultra-widefield (UWF) imaging has transformed the detection and monitoring of retinal lesions in VHL, particularly during asymptomatic stages.[8] By offering comprehensive visualization of the retinal periphery, UWF imaging significantly enhances the sensitivity of RH diagnosis.[9] However, its relatively recent adoption in clinical practice has restricted its use in prospective studies exploring the longitudinal progression, complications, and visual outcomes associated with RHs.

This study employs UWF imaging to comprehensively assess the longitudinal progression of RHs in VHL syndrome. The objectives are to evaluate the rate of new lesion formation, identify risk factors (e.g., demographics, genetic mutations, and UWF imaging features) of RHs recurrence, and document complications such as retinal detachment (RD), a leading cause of irreversible vision loss.[10] Additionally, the study quantifies the visual burden of VHL, focusing on the prevalence of blindness (visual acuity [VA] worse than 3/60[11]), moderate to severe vision impairment (VA worse than 6/18 but better than 3/60[11]), and mild vision impairment (VA worse than 6/12 but better than 6/18[11]).

Methods

This single-center longitudinal cohort study was conducted at San Raffaele Hospital, focusing on patients diagnosed with VHL syndrome. Recruitment began in January 2004, and, from 2020, participants were enrolled in a comprehensive multisystem evaluation protocol (Ospedale San Raffaele VHL Program). This protocol was managed by a multidisciplinary team of specialists in urology, neurosurgery, neuroradiology, surgical oncology, genetics, and ophthalmology.[12,13] The study complied with the Declaration of Helsinki and received institutional review board approval from San Raffaele Hospital. Written informed consent was obtained from all participants enrolled in the institutional VHL program ("protocol RENE - version 29/08/2007 - Ospedale San Raffaele di Milano") after explaining the study's objectives and methodology.

The inclusion criteria required a confirmed diagnosis of VHL syndrome, established through genetic analysis, family history, or key clinical features such as RHs, CNS hemangioblastomas, pheochromocytomas, neuroendocrine tumors, or clear cell renal carcinoma;[14] age of $\geq$18 years; a minimum follow-up period of 12 months. The exclusion criteria were severe cataracts or media opacity impairing imaging and coexisting retinal conditions such as diabetic retinopathy, uveitis, or glaucoma to minimize confounding factors. Eyes with advanced disease at baseline were also excluded, such as those with enucleation, phthisis, or total RD, as RH progression and associated characteristics could not be evaluated.

Baseline evaluations included best-corrected VA (BCVA) measurement using decimal charts, slit lamp biomicroscopy, and fluorescein angiography (FA). Imaging initially relied on a Heidelberg system with a 55° lens and peripheral steering for retinal periphery visualization, transitioning to UWF imaging (Silverstone, Optos PLC) for subsequent evaluations. Additional imaging modalities included UWF pseudocolor fundus retinal images and green-light fundus autofluorescence. For patients recruited before 2014, annual imaging was conducted using the Topcon TRC-50DX, Type IA retinal camera (Topcon) with a Nikon D7000, 16.2 Megapixel camera. From 2014 onward, these patients underwent UWF imaging for follow-up assessments.

Annual imaging and follow-up visits were conducted in accordance with established guidelines.[8] At each visit, data collected at the eye level included ocular history, BCVA, tumor counts, anatomical location, and complications such as RD, ocular phthisis, and neovascular glaucoma. Cumulative lesion counts were calculated, and tumor involvement was categorized as unilateral, bilateral, or absent. Best-corrected VA measurements were converted to logarithm of the minimum angle of resolution (logMAR), excluding values worse than 1.6 logMAR (Snellen equivalent: 20/800) from analysis.[15] Both eyes were included if eligibility criteria were met.

Treatment adhered to a multidisciplinary framework.[8,13] Extramacular and extrapapillary RHs were treated with laser photocoagulation or cryotherapy.[16] Intravitreal anti-VEGF agents injections (bevacizumab, ranibizumab, and aflibercept) were administered based on physician judgment. Advanced cases, such as exudative or tractional RD and fibrovascular proliferation, were treated with pars plana vitrectomy (PPV).[17] No systemic therapy, including belzutifan, was administered either before or during the study period.

Multimodal Imaging Analysis

Retinal hemangioblastomas were categorized into 3 anatomical regions[7]: (1) juxtapapillary, within half a disc diameter from the optic nerve; (2) macular, within half a disc diameter from the foveola; and (3) peripheral, encompassing all other regions. Juxtapapillary and macular RHs were grouped as central RHs. Peripheral RHs were further classified as[18] superotemporal, inferotemporal, superonasal, and inferonasal. To achieve accurate classification, UWF color fundus images were overlaid with a digitally generated segmentation grid representing the 7 standard ETDRS fields, allowing precise evaluation of RHs distribution across the extended fields (Fig 1).

Fluorescein angiography identified segmental diffuse vascular leakage as late-phase leakage from second-order or more peripheral retinal veins and adjacent capillaries, regardless of RH presence.[19] ; and foveal hardexudation, assessed via FA and OCT, were evaluated as markers of active retinal edema or chronic lipid deposition (Fig 2).

Genetic Characterization

We collected results from genetic analysis performed on genomic DNA extracted peripheral blood monocytes. Targeted next-generation sequencing was used to detect single nucleotide variants and small insertions or deletions, and Multiplex Ligation-dependent Probe Amplification to detect copy number variants. Germline variants in the *VHL* gene were interpreted according to the American College of Medical Genetics and Genomics guidelines and classified according to their predicted coding impact as missense or null variants (including nonsense, frameshift, splice site, and exon deletions).[20]

Statistical Analysis

All statistical analyses were performed using R (version 4.4.2). Statistical significance was set at $\alpha < 0.05$, and all tests were 2-

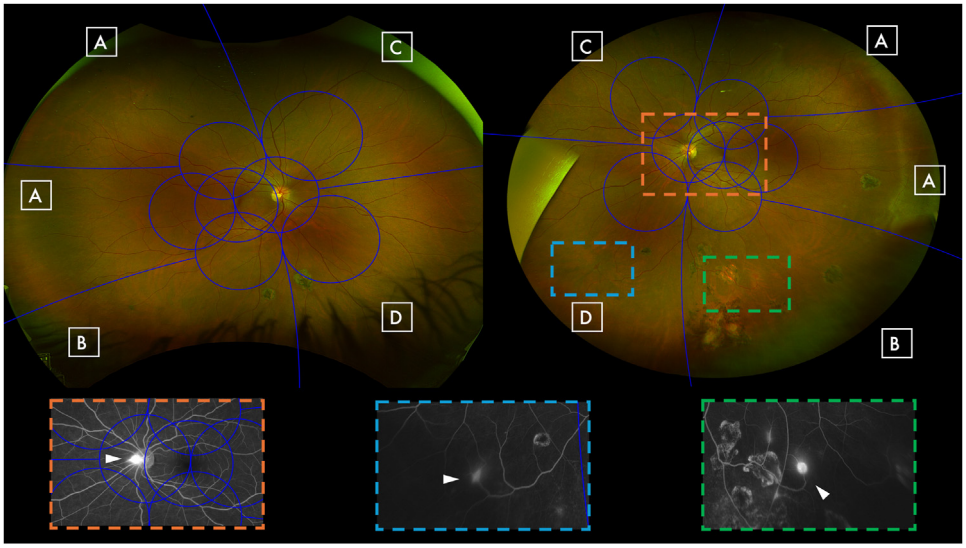

Figure 1. Segmentation of extended fields in UWF and UWF FA imaging. This image depicts the UWF color fundus images of 2 eyes from a patient affected by VHL disease. A digitally generated overlay representing the 7 standard ETDRS fields was aligned with each image based on the specific anatomical locations of the foveola and the optic nerve head. This overlay was used to evaluate the distribution of retinal lesions within modified extended fields derived from the UWF images. In the image, the regions labeled "**A**" correspond to the superior temporal field, "**B**" to the inferior temporal field, "**C**" to the superior nasal field, and "**D**" to the inferior nasal field. The lower colored boxes represent UWF FA images highlighting RHs, each indicated by arrowheads. The orange box corresponds to a RH located at the optic nerve head, as shown by the arrowhead. The blue box displays a RH in the inferior nasal field, whereas the green box highlights a RH in the inferior temporal field. These angiographic findings illustrate the precise localization of retinal lesions characteristic of VHL disease. FA = fluorescein angiography; RD = retinal detachment; UWF = ultra-widefield; VA = visual acuity; VHL = von Hippel–Lindau.

sided. Continuous variables were summarized as means with standard deviations or medians with interquartile ranges, whereas categorical variables were reported as frequencies and percentages.

The primary outcomes were the cumulative incidence of new RHs. Kaplan–Meier survival analysis was used to analyze time-to-event data and estimate cumulative incidence. The

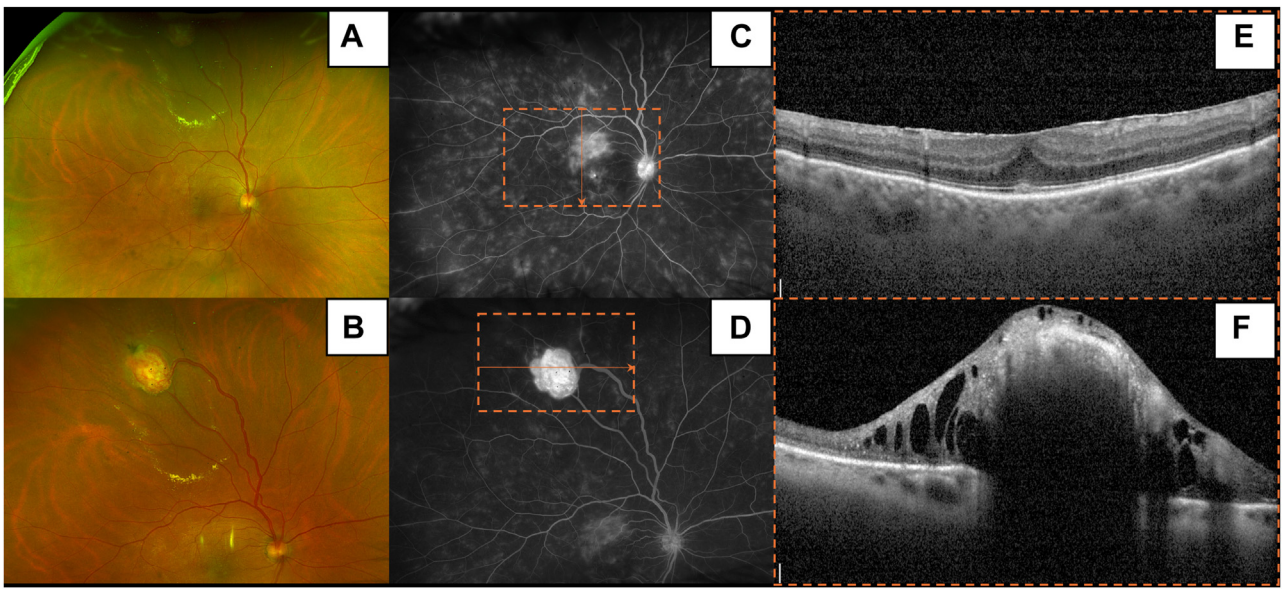

Figure 2. Multimodal imaging of a RH in the superior temporal quadrant. Panels (**A**) and (**B**) show pseudocolor fundus images, highlighting a large RH in the superior temporal quadrant, with well-defined afferent and efferent vascular components. Above the superior vascular arcade, yellowish material is visible, consistent with retinal hard exudation. Panels (**C**) and (**D**) present UWF FA images, demonstrating hyperfluorescence at the RH site, corresponding to the lesion. Additionally, areas of diffuse and segmental vascular leakage and macular hyperfluorescence are evident. Panel (**E**) displays the macular OCT, revealing the presence of an epiretinal membrane. Panel (**F**) shows an OCT scan centered on the RH, demonstrating IRF, retinal exudation, and a hyperreflective intraretinal mass corresponding to the RH. Orange box represents a zoomed-in view of the corresponding area in the lower left corner. FA = fluorescein angiography; IRF = intraretinal fluid; RH = retinal hemangioblastoma; UWF = ultra-widefield.

incidence rate of new RH, defined as the number of new events per unit of person-time at risk, was calculated by dividing the total number of new RHs by the total person-time at risk. This rate was further analyzed using a mixed-effects negative binomial regression model, which included follow-up time as an offset to account for varying observation periods. Random intercepts for patients and eyes were incorporated to address the hierarchical structure of the data and the correlation between eyes within the same patient.

Univariable analyses were initially performed to assess individual predictors. Variables with a P value ≤ 0.1 were considered for inclusion in the multivariable model. Results were reported as incidence rate ratios (IRRs), quantifying the relative change in the incidence rate of new RHs per unit or category change in a predictor variable. Incidence rate ratios greater than 1 indicated an increased rate, whereas IRRs <1 suggested a reduction. For example, an IRR of 1.50 reflected a 50% increase, whereas an IRR of 0.75 represented a 25% reduction. Residual diagnostics, conducted using the DiagnosticsforHierArchicalRegressionModels package, confirmed the suitability of the negative binomial framework and ruled out overdispersion. Alternative models, including Poisson and zero-inflated negative binomial regressions, were evaluated but did not outperform the primary model based on Akaike Information Criterion comparisons.

Sensitivity analyses were conducted to assess hazard of recurrent RHs using the Andersen–Gill extension of the Cox proportional hazards model, which incorporated frailty terms to account for repeated measures within the same eye and clustering at the patient level. These models provided time-dependent hazard estimates for RH recurrence, complementing the primary analysis. Proportional hazards assumptions were tested with Schoenfeld residuals, and univariable survival models were applied to individual predictors. Concordance between survival models and the negative binomial regression further supported the robustness and reliability of the findings.

Results

Study Population and Baseline Patients' Characteristics

A total of 112 eyes from 56 patients were initially included. Thirty-three eyes were excluded due to advanced disease at baseline, comprising 4 enucleated eyes, 9 with ocular phthisis, and 6 with RD. Fourteen additional eyes were excluded because RHs could not be reliably assessed. Among the 33 eyes excluded, the mean age at baseline was 44.1 $\pm$ 10.34 years, with a mean follow-up duration of 60.74 $\pm$ 47.21 months. Regarding genetic analysis, data were unavailable for 4 patients. Among the remaining 29 eyes, 17 (59%) harbored a missense variant, whereas 12 (41%) carried a null variant, including 8 (28%) nonsense mutations and 4 (13%) exon deletions. In our cohort, RHs were the initial manifestation of VHL disease in 20 out of 43 patients (47%), whereas in another 20 cases (47%), they developed as a secondary manifestation. The remaining 3 patients (6%) were disease-free.

The final cohort comprised 43 patients (78 eyes), with 23 male participants (54%). All patients were Caucasian and represented 31 distinct family clusters. The mean age at baseline was 47.8 $\pm$ 13.6 years. The median follow-up duration was 30.75 months (interquartile range: 27–109 months). Each patient underwent a median of 4 visits (interquartile range: 3–10).

von Hippel–Lindau variants were identified in all participants: 19 (51%) were missense, 10 nonsense (27%), 1 (3%) frameshift, 1 (3%) splice site, and 6 (16%) exon deletions. Genetic data were unavailable for 6 participants. Overall, the proportion of patients harboring missense alleles (19 of 37; 51%) or presumed null alleles was similar (18 of 37; 49%). Three of 18 unique variants (17%) were previously not reported in the literature. A detailed assessment of identified variants is provided in a Table 1. Baseline demographic and clinical characteristics are summarized in Table 2A.

Distribution of New RHs

At baseline, 110 RHs were documented (Fig 3), with 39 eyes (49%) showing no RHs, 5 eyes (6%) exhibiting central RHs, 28 eyes (35%) having peripheral RHs, and 6 eyes (10%) presenting with both central and peripheral RHs (Table 2B). During the follow-up, 86 new RHs were identified, 2% central and 98% peripheral, distributed as follows: 33 (38%) superotemporal, 21 (24%) inferotemporal, 16 (19%) superonasal, and 16 (19%) inferonasal (Fig 4).

By the last available examination, 26 eyes (34%) remained disease-free, 17 (23%) showed no progression of existing RHs, and 35 (43%) developed new RH.

Tumor laterality also evolved significantly ($P = 0.004$). Initially, 8 (19%) of patients had bilateral RHs, 15 (35%) unilateral RHs, and 20 (46%) no RHs. By study end, these percentages shifted to 15 (35%), 22 (51%), and 6 (14%), respectively.

Incidence and Risk Factors of New RHs

The overall incidence rate of new RHs was 0.22 per eye-year (95% confidence interval [CI]: 0.17–0.27), equating to 1 new RH per eye every 5 years (Fig 5). Mixed-effects negative binomial regression revealed no significant temporal change in incidence ($\beta = 0.0021$, $P = 0.5$), but substantial variability existed at the eye (variance = 0.58) and patient (variance = 0.20) levels.

Univariable analysis identified older age as protective, reducing the IRR of new RHs by 3.3% annually ($P = 0.013$, Table 3). Baseline tumors in the same eye reduced the IRR by 81% ($P = 0.03$), whereas higher tumor counts increased the IRR by 29% per additional lesion ($P < 0.001$). Segmental diffuse vascular leakage significantly elevated the IRR by 172% ($P = 0.03$). The presence of bilateral tumors showed a 151% higher IRR compared to unilateral tumors ($P = 0.06$). Other factors, including central lesions, IRF, exudation, and variants type, did not demonstrate significant associations with the incidence of new RHs. Multivariable analysis confirmed these findings, showing a 4.2% annual reduction in IRR with age ($P = 0.003$) and an 89% increase associated with vascular leakage (P=0.004).

Table 1. Summary of all Unique VHL Variants Identified in the Study Cohort, In Silico Pathogenicity Scores, and Classification Criteria

Genomic Position (hg38)	cDNA Variant (NM_000551.4)	Protein Variant (NP_000542.1)	Coding Impact	Location	dbSNP	Number of Alleles in the Current Study	ACMG Classification	Allele Frequency (gnomAD v4.0.0)	Metadome Tolerance Score	Revel	PhyloP100 Conservation Score	MetaRNN	Alpha Missense	Reference
chr3-10142041-C-A	c.194C>A	p.(Ser65*)	Nonsense	Exon 1 of 3 position 264 of 410	rs5030826	1	Pathogenic	-	-	-	-	-	-	Whaley JM et al 1994 (PMID: 7977367)
chr3-10142080-A-G	c.233A>G	p.(Asn78Ser)	Missense	Exon 1 of 3 position 303 of 410	rs5030804	3	Pathogenic	-	0.4	0.767	5.718	0.9908	0.881	Chen et al 1995 (PMID: 7728151)
chr3-10142109-T-G	c.262T>G	p.(Trp88Gly)	Missense	Exon 1 of 3 position 332 of 410	-	1	Pathogenic	-	0.54	0.89	-	0.9914	0.99	Chen et al 1995 (PMID: 7728151)
chr3-10142173-T-	c.326del	p.(Ile109Thrfs*50)	Frameshift	Exon 1 of 3 position 396 of 410	-	1	Pathogenic	-	-	-	-	-	-	Novel
chr3-10142180-C-G	c.333C>G	p.(Ser111Arg)	Missense	Exon 1 of 3 position 403 of 410	rs765978945	3	Pathogenic	-	0.15	0.798	1.758	0.9637	0.999	Chen et al 1995 (PMID: 7728151)
chr3-10146516-C-T	c.343C>T	p.(His115Tyr)	Missense	Exon 2 of 3 position 3 of 123	rs5030811	1	Pathogenic	-	-	-	-	-	-	Novel
chr3-10146580-T-C	c.407T>C	p.(Phe136Ser)	Missense	Exon 2 of 3 position 67 of 123	rs5030833	1	Pathogenic	-	0.7	0.802	4.404	0.9946	0.996	Martin et al 1998 (PMID: 1062 7136)
chr3-10146618-G-A	c.445G>A	p.(Ala149Thr)	Missense	Exon 2 of 3 position 105 of 123	rs587780077	1	Pathogenic	-	0.96	0.861	7.677	0.9899	0.823	Crossey et al 1994 (PMID: 7987306)
chr3-10146639-A-T	c.463+3A>T	p.(?)	Splice site	Intron 2 of 2 position 3 of 3150	rs1131690954	1	Pathogenic	-	-	-	4.344	-	-	Novel
chr3-10149822-C-T	c.499C>T	p.(Arg167Trp)	Missense	Exon 3 of 3 position 36 of 3881	rs5030820	7	Pathogenic	-	-	0.868	3.372	0.9922	0.932	Zbar et al 1996 (PMID: 8956040)
chr3-10149823-G-A	c.500G>A	p.(Arg167Gln)	Missense	Exon 3 of 3 position 37 of 3881	rs5030821	1	Pathogenic	-	0.6	0.874	7.779	0.9921	0.879	Zbar et al 1996 (PMID: 895 6040)
chr3-10149840-G-T	c.517G>T	p.(Glu173*)	Nonsense	Exon 3 of 3 position 54 of 3881	rs1575932228	7	Pathogenic	-	-	-	-	-	-	Mandich et al 1998 (PMID: 9452 106)
chr3-10149848-C-G	c.525C>G	p.(Tyr175*)	Nonsense	Exon 3 of 3 position 62 of 3881	rs5030835	1	Pathogenic	-	-	-	-	-	-	Olschwang et al (PMID: 9829912)
chr3-10149886-T-C	c.563T>C	p.(Leu188Pro)	Missense	Exon 3 of 3 position 100 of 3881	rs1559429824	1	Pathogenic	-	0.8	0.959	6.258	0.9912	0.996	Martin et al 1998 (PMID: 1062 7136)
chr3-10149906-C-T	c.583C>T	p.(Gln195*)	Nonsense	Exon 3 of 3 position 120 of 3881	rs5030825	1	Pathogenic	-	-	-	-	-	-	Crossey et al 1994 (PMID: 7987 306)
-	Exon 1 deletion	p.(?)	Deletion			1		-	-	-	-	-	-	-
-	Exon 1-2 deletion	p.(?)	Deletion			3		-	-	-	-	-	-	-
-	Exon 1-3 deletion	p.(?)	Deletion			2		-	-	-	-	-	-	-

In an amino acid sequence, an asterisk (*) represents a stop codon. This means the end of the protein coding sequence — it's where the ribosome stops translating the mRNA into a protein.
ACMG = American College of Medical Genetics and Genomics; dbSNP = Database of Single Nucleotide Polymorphisms; PMID = PubMed Identifier.

Table 2. Clinical Characteristics of Patients and Eyes. A. Demographic and Genetic Status of Included Patients. B. Clinical and Morphologic Characteristics of Eyes Grouped by RHs Status at Baseline

A	Overall (N = 43 Patients)
Age (years)	
Mean (SD)	47.8 (13.6)
Median [min, max]	50.0 (19.0, 74.0)
Male gender	23 (54%)
RHs baseline status	
Bilateral tumors	8 (19%)
Unilateral tumors	15 (35%)
No tumors	20 (46%)

B	Overall (n = 78 Eyes)	No RHs (n = 39 Eyes)	Central RHs (n = 5 Eyes)	Peripheral RHs (n = 28 Eyes)	Both RHs (n = 6 Eyes)
Baseline BCVA (logMAR)	0.05 (0.2)	0.05 (0.18)	0.25 (0.25)	0.02 (0.06)	0.24 (0.47)
Intraretinal fluid	3 (4%)	0 (0%)	0	1 (1%)	2 (3%)
Exudation	4 (5%)	0 (0%)	0	2 (2.5%)	2 (2.5%)
Segmental diffuse vascular leakage	5 (6%)	0 (0%)	0	4 (5%)	1 (1%)

BCVA = best-corrected visual acuity; logMAR = logarithm of the minimum angle of resolution; RH = retinal hmangioblastoma; SD = standard deviation.

Risk Factors for Recurrent RHs

Cox frailty models highlighted key risk factors for recurrent RHs. Age remained protective (hazard ratio [HR] = 0.96, $P = 0.018$), whereas prior lesions significantly reduced the hazard of recurrence (HR = 0.11, $P = 0.033$). Peripheral lesions were the strongest predictor of increased recurrence risk (HR = 16.38, $P < 0.001$). The multivariable model confirmed the protective role of age (HR = 0.97, $P = 0.04$) and suggested a trend toward reduced risk with unilateral tumor involvement (HR = 0.30, $P = 0.06$).

Longitudinal Visual Change, Complications, and Treatment

The mean BCVA (logMAR) worsened from 0.05 ± 0.2 (Snellen equivalent: 20/22) at baseline to 0.11 ± 0.3 (Snellen equivalent 20/25) at follow-up, with a decline of + 0.014 logMAR per year (95% CI: 0.010−0.020; $P < 0.001$). During the follow-up, 59 eyes (75%) maintained stable vision, whereas 20 eyes (25%) experienced vision deterioration, of which 16 (80%) presented at baseline or develop at least 1 RH during the follow-up. Among these, 2 patients (5%) developed blindness in 1 eye (due to ocular phthisis and RD), 2 (5%) developed moderate to severe vision impairment (due to IRF and hard exudation), and 3 (7%) developed mild vision impairment.

Management included retinal laser photocoagulation (33 [42%] eyes of 25 [58%] patients underwent laser treatment during follow-up (Fig 6), with an average 0.40 ± 0.72 sessions per eye per year), anti-VEGF injections (6 [8%] eyes of 6 [14%] patients), and PPV for RD (2 [3%] eyes of 2 [5%] patients). Of these 6 eyes, 4 exhibited RH progression during follow-up. None of the patients developed neovascular glaucoma.

Discussion

This study provides a comprehensive analysis of ocular VHL disease, focusing on demographics, incidence, and visual outcomes of RHs, with UWF imaging offering enhanced detection. By documenting the rate of new RH formation, identifying risk factors, and analyzing complications such as RD, this study delivers valuable insights into the burden of RHs. To our knowledge, this is the first study to assess the long-term progression of ocular VHL using UWF imaging, establishing a foundation for improved management strategies. Moreover, our cohort represents the natural history of VHL disease in the absence of systemic therapy, which is not yet approved in the European Union.[21–23]

The cohort, comprising 78 eyes, demonstrated significant variability in disease severity and natural history, with a quarter of patients followed for more than 9 years. Although 46% of patients were disease-free at baseline, only 34% remained so during follow-up, whereas 43% developed new lesions. The progression rate surpassed prior reports (e.g., 27% by Wong et al[5] and 28% by Dollfus et al[24]) likely due to the superior sensitivity of

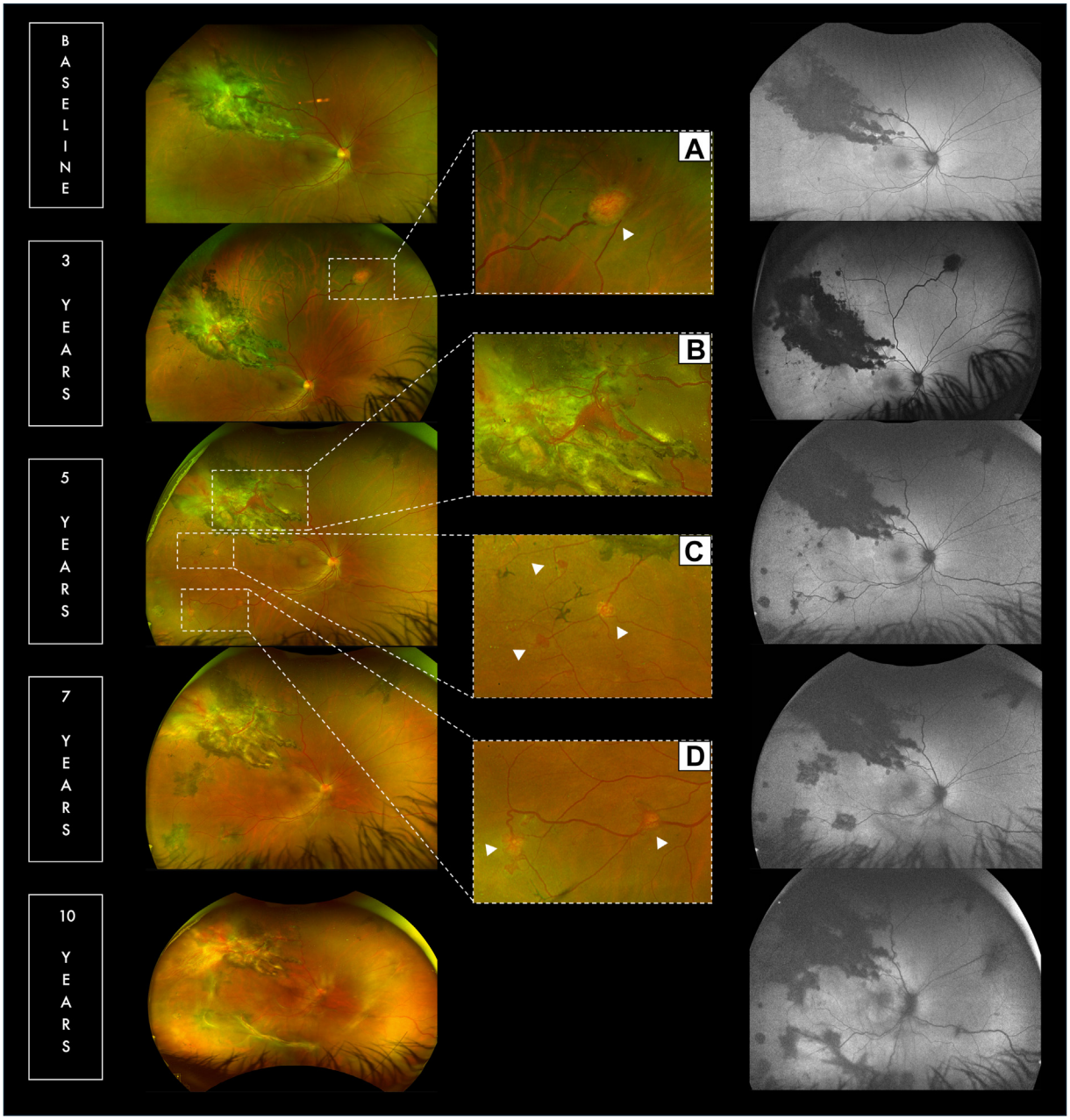

Figure 3. Long-term UWF imaging follow-up of RHs in VHL disease. This figure illustrates a long-term clinical follow-up of the right eye of a female patient with VHL disease, monitored through UWF imaging. At baseline, the patient was 28 years old and had previously undergone retinal laser photocoagulation for a RH located in the superior temporal field. The treated lesion exhibited a fibrotic and atrophic appearance, corresponding to a hypoautofluorescent area on the BAF imaging. During the follow-up, the patient developed 9 additional RHs. Among these, by the third year, a prominent ovoidal RH emerged in the superior nasal quadrant (**A**), characterized by a yellowish mass with afferent and efferent vascular components. Several smaller RHs developed by the fifth year (**C** and **D**), absent at baseline. Notably, a recurrence of the previously treated RH in the superior temporal quadrant was observed by the third year, signifying reactivation of the lesion (**B**). New RHs are indicated by white arrowheads. By the 7-year follow-up, areas of atrophy had developed around the angiomatous lesions, secondary to the laser photocoagulation treatment. At the 10-year mark, diffuse retinal damage became apparent, with extensive fibrotic changes observed across the retina. These alterations contributed to significant visual deterioration. By the end of the follow-up period, the patient's BCVA declined from a baseline of 0.1 logMAR to 0.7 logMAR. BAF = blue autofluorescence; BCVA = best-corrected visual acuity; logMAR = logarithm of the minimum angle of resolution; RH = retinal hemangioblastoma; UWF = ultra-widefield; VHL = von Hippel–Lindau.

UWF imaging in detecting peripheral and smaller RHs and the regular annual follow-up with FA. Chen et al,[9] for instance, showed that two-thirds of RHs identified via UWF FA were missed by conventional fundoscopy, underscoring the importance of advanced imaging in detecting subtle peripheral lesions. The overall incidence

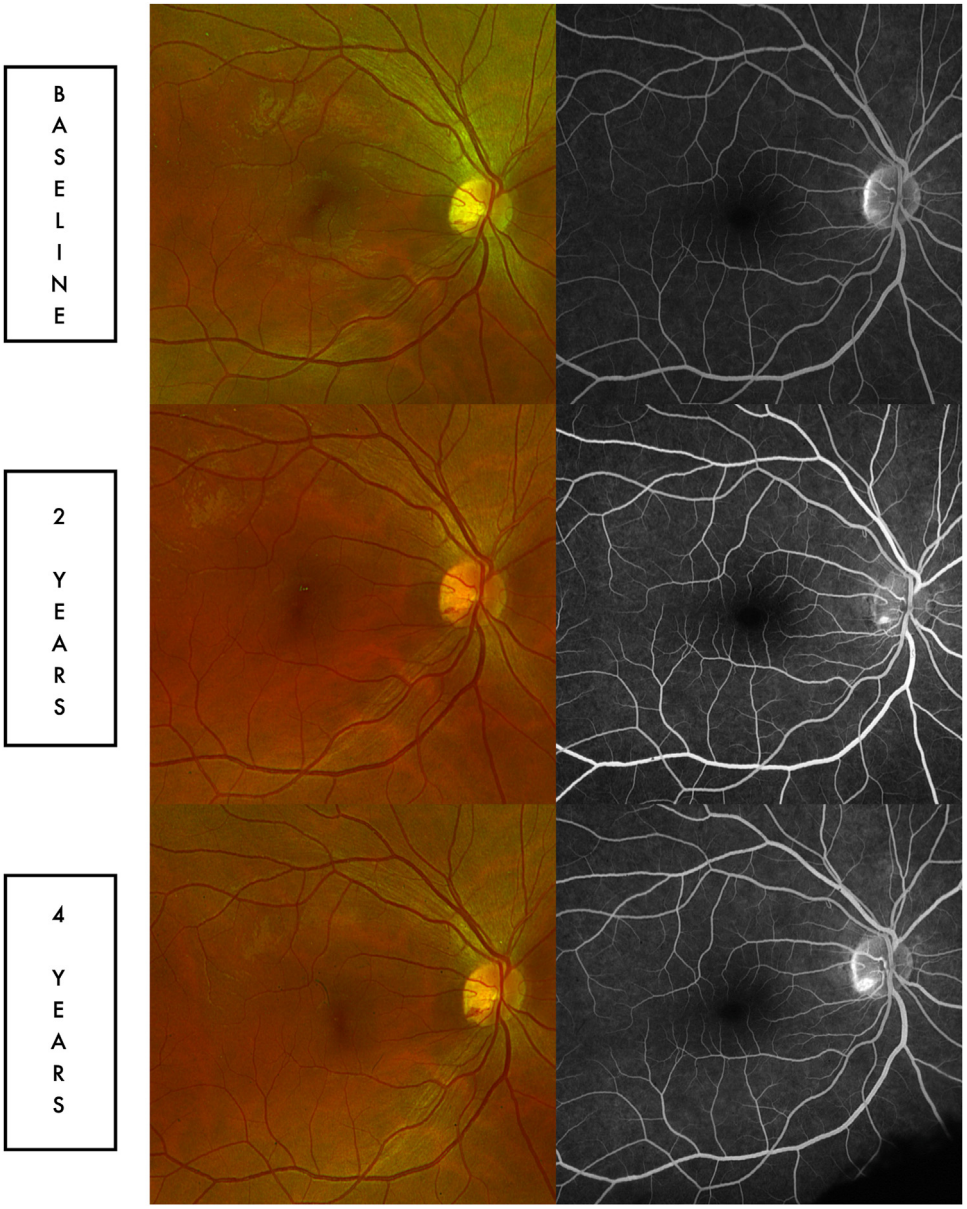

Figure 4. Longitudinal follow-up of a patient with the development of a juxtapapillary RH in the right eye. At baseline, the patient was 27 years old and had previously undergone treatment for other RHs. During the follow-up period, 3 additional RHs developed. The Optos pseudocolor fundus retinal images reveal the progressive appearance of a small reddish lesion at the inferotemporal margin of the optic disc over time. At baseline, FA showed no evidence of leakage during the early phases. In contrast, at the end of the follow-up period, increasing leakage is evident in the early phases of FA, highlighting the progression of the juxtapapillary hemangioblastoma. Notably, no changes in visual acuity were observed throughout the follow-up period. FA = fluorescein angiography; RH = retinal hemangioblastoma.

rate of 0.22 RHs per eye-year—equivalent to 1 new tumor per eye every 5 years—highlights the persistent risk of RH development, with no significant temporal change observed at a population level.

Older age emerged as a protective factor, reducing the IRR of new RHs by 4.2% annually, consistent with previous findings that disease activity diminishes over time. Kreusel et al,[25] for example, noted that patients >50 years of age were less prone to develop new RHs. This supports the adoption of tailored follow-up strategies, with younger patients requiring more frequent monitoring. Conversely, cumulative tumor burden expressed as higher tumor counts, was strongly linked to higher RH incidence, reflecting the role of microenvironmental changes, such as hypoxia and vascular instability, in promoting angiogenesis.[26–29] Vascular leakage, associated with a 172% increase in IRR of new RHs, emerged as a potential predictive marker; in keeping with this, biallelic inactivation of the *VHL* gene in retinal cells has been shown to increase vascular permeability and promote hemangioblastoma-like lesions,

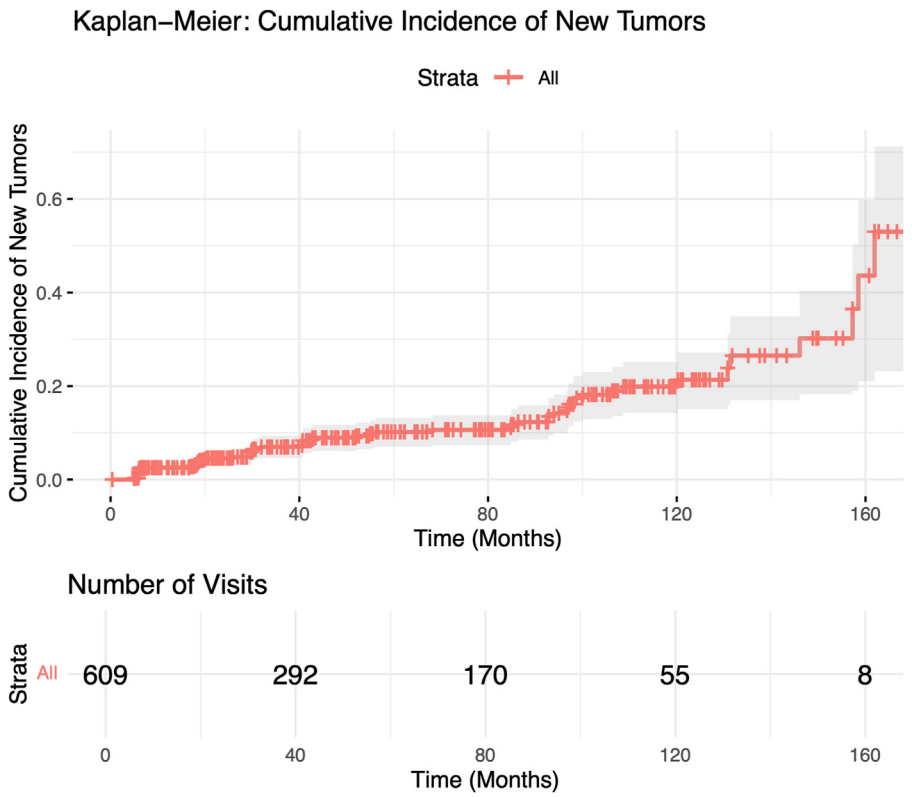

Figure 5. Kaplan–Meier survival curve showing the cumulative incidence of new RHs over time. This Kaplan–Meier curve illustrates the cumulative incidence of new RHs over time for all eyes included in the study. The analysis encompasses a total of 609 visits available for all eyes, with follow-up durations ranging up to 160 months. The number of eyes at risk decreases over time, as indicated by the counts displayed below the timeline. RH = retinal hemangioblastoma.

reinforcing a proangiogenic environment.[26–29] Finally, baseline RHs in the same eye exhibited a protective effect, reducing the IRR by >80%, even though an indirect effect of age on this finding cannot be excluded.

The sensitivity analysis using Cox proportional hazards models with frailty provided insights into the risk of recurrent RHs using a survival statistical approach. Notably, age was confirmed as a significant protective factor, with

Table 3. Factors Associated with the IRR of New RHs

Variable	Estimate	Percentage Effect on IRR (Exponential)	95% CI	*P* Value
Age (for each year)	−0.033	−3.3	−0.06 to −0.01	0.013*
Male gender (ref: female)	−0.311	−26.8	−1.09 to 0.47	0.4
Null *VHL* variants (vs. missense variants)	0.159	17.3	−1.17 to 1.49	0.812
Bilateral tumors (vs. unilateral tumors)	0.920	151	−0.05 to 1.88	0.06*
Baseline BCVA (for each logMAR)	0.143	15.3	−0.72 to 1.004	0.7
Presence of any tumor at baseline in the same eye (ref: no)	0.099	10.5	−0.62 to 082	0.5
Number of tumors in the same eye (for each lesion)	0.02	29	−0.09 to 0.12	0.7
Central lesions (vs. peripheral lesions)	0.648	91.3	−0.15 to 1.44	0.11
Intraretinal fluid (vs. no)	−0.162	−19.7	−1.27 to 0.91	0.6
Exudation (vs. no)	−0.531	−37.7	−1.52 to 0.68	0.5
Segmental diffuse vascular leakage (vs. no)	1.002	172.3	0.06–1.94	0.03*

BCVA = best-corrected visual acuity; CI = confidence interval; IRR = incidence rate ratio; logMAR = logarithm of the minimum angle of resolution; RH = retinal hemangioblastoma; VHL = von Hippel–Lindau.
The Table 3 summarizes the results of the univariable analysis assessing the impact of various predictors on the incidence of new RHs. For each variable, the estimated effect on the IRR, expressed as the percent change, along with the 95% confidence interval and *P* value, is provided. A negative percentage indicates a protective factor, whereas a positive percentage reflects an increased risk of RH development.
*Significant associations ($P < 0.05$).

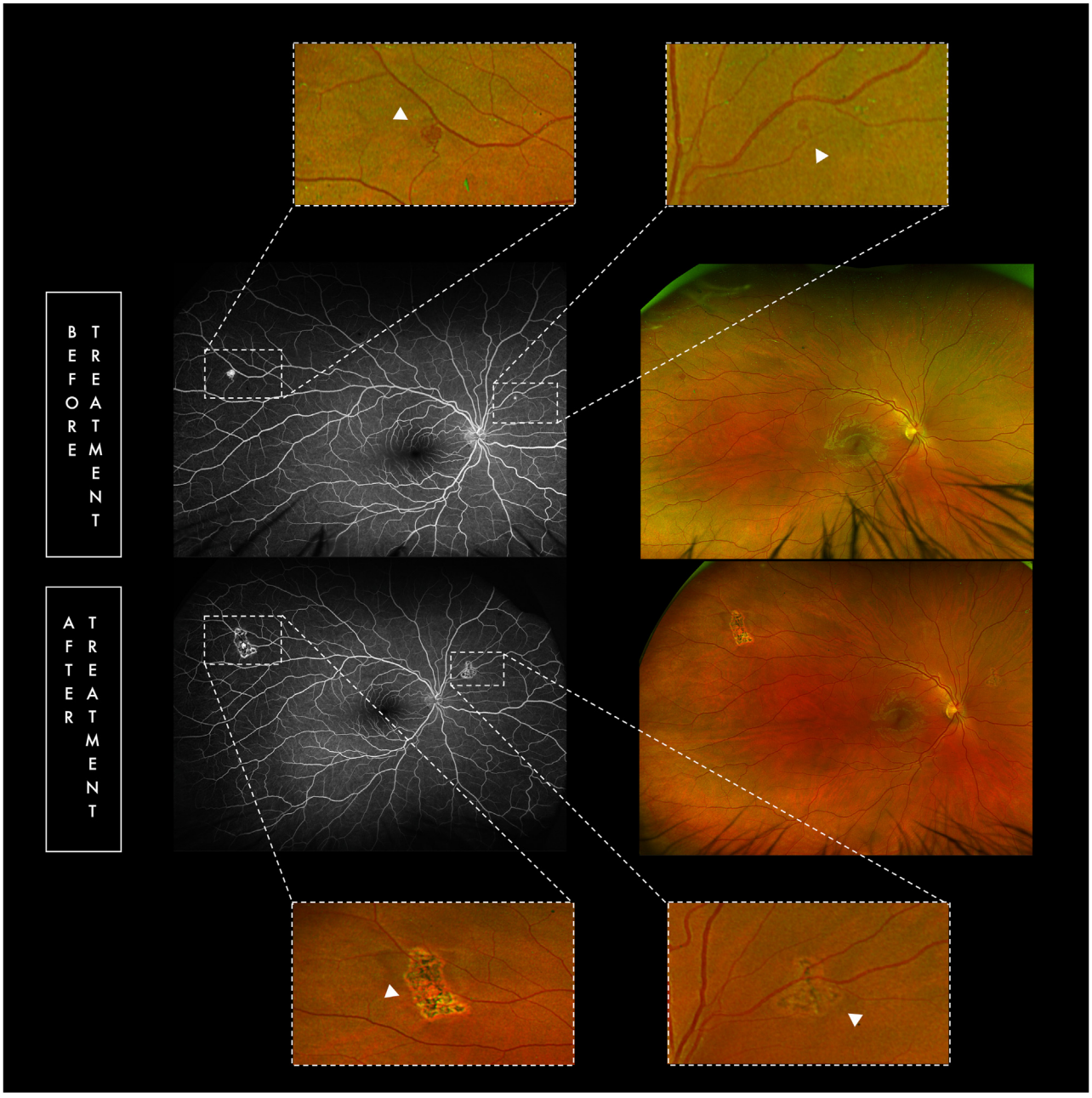

Figure 6. Ultra-widefield FA and Optos pseudocolor fundus retinal imaging before and after laser photocoagulation treatment of RH. The central panels show UWF FA (left) and Optos pseudocolor fundus retinal images (right) of the retina before and after treatment. Two small RHs are identified on FA: one in the superior temporal field and the other in the superior nasal field. These small lesions are more challenging to detect on Optos pseudocolor fundus retinal imaging, as highlighted in the magnified views at the top. After treatment, UWF FA images reveal hypoautofluorescent areas at the site of the treated lesions. The magnified views at the bottom better illustrate these atrophic changes, which are more distinctly visible posttreatment. The arrowheads indicate areas of atrophy within the zoomed-in regions, which are highlighted by white boxes in the figure. FA = fluorescein angiography; RH = retinal hemangioblastoma; UWF = ultra-widefield.

each additional year reducing the hazard of new RHs. Peripheral involvement was a significant risk factor for recurrence, increasing the hazard by >15 times. The observed predilection for recurrence in peripheral lesions likely reflects a combination of both biological and clinical factors. From a biological perspective, the peripheral retina may be inherently more susceptible to proangiogenic stimuli due to its lower vascular density, reduced autoregulatory capacity, and increased vulnerability to subclinical ischemia.[30] This hypothesis is supported by UWF studies in VHL disease itself as well as in other retinal vascular disorders, such as diabetic retinopathy and sickle cell retinopathy, in which peripheral ischemia has been associated with neovascularization at the retinal periphery,

particularly along the vascular arcades.[31] In contrast, posterior pole ischemia has been more consistently linked to optic disc neovascularization.[32,33] In the context of VHL, chronic peripheral hypoxia may amplify the effects of constitutive hypoxia-inducible factor activation, fostering a permissive proangiogenic microenvironment that facilitates tumor recurrence in the peripheral retina. As previously demonstrated,[34] stromal cells within RHs exhibit biallelic VHL gene inactivation and elevated VEGF expression, promoting neovascularization in the surrounding tissue. The significantly higher recurrence risk associated with peripheral tumor involvement may therefore be partly explained by this localized VEGF upregulation. Further supporting this hypothesis is evidence of peripheral vascular leakage in VHL eyes, indicative of ongoing vascular instability.[19] In addition to these biological considerations, clinical factors may also play a significant role. Peripheral RHs are often more difficult to detect early and may be less completely or less aggressively treated than centrally located lesions, particularly in the absence of UWF or when peripheral visualization is suboptimal. As a result, these tumors may have a higher likelihood of residual activity or regrowth. The presence of RHs at baseline in the same eye again showed a protective effect on the hazard of developing new lesions.

Interestingly, this study did not identify a significant difference in the risk of RH progression between null variants and missense variants of the *VHL* gene. This finding aligns with previous evidence suggesting that, although null variants are often associated with more severe systemic manifestations of VHL syndrome, their impact on ocular phenotypes may be less pronounced.[8,29] It is possible that the localized retinal microenvironment and other modifier factors, play a more critical role in driving RH progression. Future studies incorporating larger cohorts and detailed genetic characterization could further elucidate these genotype-phenotype correlations.

Visual outcomes remain a critical concern in ocular VHL disease as the progressive nature of the condition poses significant challenges to maintaining good vision. The visual burden of ocular VHL disease remains substantial, with the mean BCVA declining from 0.05 (Snellen equivalent: 20/22) to 0.11 (Snellen equivalent: 20/25) logMAR over the follow-up, reflecting the chronic progression of the disease. Although 75% of eyes maintained stable vision, 25% exhibited deterioration, primarily due to complications secondary to RHs, with 5% progressing to blindness. These findings align with prior reports,[5] emphasizing the rarity of severe visual impairment when timely interventions are applied.

Laser photocoagulation remains the primary treatment for extramacular and extrapapillary RHs, consistent with established guidelines.[8] Small RHs (<1.5 mm) were managed effectively with single-session treatments, as reported by Krivosic[16] and Singh et al[6] in separate cohorts. However, posterior RHs near the optic disc or macula lack safe and effective treatment options. Further longitudinal studies are needed to identify the best management for these rare, sight-threatening RH locations.

This study's strengths include its robust cohort, extended follow-up, and the use of UWF imaging for comprehensive lesion analysis. However, limitations such as its retrospective design, exclusion of eyes with advanced disease, and potential selection bias may limit generalizability. Additionally, the analyzed sample exclusively comprised individuals of Caucasian ethnicity, which may further restrict the applicability of findings to more diverse populations. Moreover, the study design required excluding cases of advanced-stage disease. This constraint may have affected the scope of the analysis, potentially limiting the ability to fully capture the spectrum of disease progression and longitudinal visual changes in VHL syndrome.

Additionally, 6 eyes received a single intravitreal injection during the follow-up. Given the short-term effect of intravitreal anti-VEGF injections (approximately 30 days) and the low number of treated eyes, we do not expect a significant impact on long-term RH recurrence rates, though this remains a study limitation. Moreover, we recognize the importance of evaluating whether systemic tumors correlate with ocular disease severity, as this may provide insights into genotype-phenotype associations. However, our study did not include an analysis of extraocular manifestations of VHL disease. The absence of systemic disease characterization limits a comprehensive assessment of potential correlations between ocular and systemic tumor burden. Future studies integrating longitudinal data on both ocular and systemic disease to better elucidate these interactions. Furthermore, 46% of patients in our cohort did not develop tumors, suggesting potential protective factors or distinct phenotypic traits. Further studies are needed to investigate these mechanisms. Finally, the relatively small number of events further constrained the statistical power of multivariable analyses.

This study highlights the recurrent nature of ocular VHL disease, underscoring the importance of early detection, individualized risk factors, and timely intervention to manage RHs and preserve vision. Future research should explore novel therapeutic strategies for posterior RHs and investigate factors contributing to disease variability and progression.

Footnotes and Disclosures

Originally received: May 28, 2025.
Final revision: May 30, 2025.
Accepted: May 30, 2025.
Available online: June 9, 2025. Manuscript no. ORET-D-25-00074.

[1] School of Medicine, Vita-Salute San Raffaele University, Milan, Italy.

[2] Ophthalmology Unit, IRCCS San Raffaele Scientific Institute, Milan, Italy.

[3] URI-Urological Research Institute, Division of Experimental Oncology, Department of Urology, IRCCS Ospedale San Raffaele, Milan, Italy.

[4] Ospedale San Raffaele VHL Program, Milan, Italy.

[5] Service of Laboratory Medicine, Molecular Genetics Service and Clinical Genomics, Milan, Italy.

Disclosure(s):

The Article Publishing Charge (APC) for this article was paid by IRCCS Ospedale San Raffaele, Milan, Italy.

All authors have completed and submitted the ICMJE disclosures form.

The authors have made the following disclosures:

A.L.: Consultant − Telix Pharmaceuticals, Alexion, Merck Sharp & Dohme.

F.B.: Consultant − Alimera Sciences (Alpharetta, GA, USA), AbbVie Inc. (North Chicago, IL, USA), Bayer Shering-Pharma (Berlin, Germany), Boehringer-Ingelheim (Ingelheim, Germany), Breye-Therapeutics (Hørsholm, Denmark), Fidia Sooft (Abano Terme, Italy), Hoffmann-La-Roche (Basel, Switzerland), Novartis (Basel, Switzerland), NTC Pharma (Milan, Italy), Oxurion NV (Leuven, Belgium), Outlook Therapeutics (Iselin, NJ, USA), Sifi (Catania, Italy).

Supported by grants from Italian Ministry of Health and the European Union for the project "CAT-VHL - Exploring the role of Carbonic Anhydrase IX as diagnostic and Theranostic target in Von Hippel−Lindau disease" (PNRR-POC-2023-12377493 [A. L.]).

HUMAN SUBJECTS: Human subjects were included in this study. The study complied with the Declaration of Helsinki and received institutional review board approval from San Raffaele Hospital. Written informed consent was obtained from all participants enrolled in the institutional VHL program ("protocol RENE - version 29/08/2007 - Ospedale San Raffaele di Milano") after explaining the study.

No animal subjects were used in this study.

Author Contributions:

Conception and design: Del Fabbro, Cicinelli

Data collection: Del Fabbro, Lattanzio, Bousyf, Bruno, Bruschi, Arrigo, Pipitone, Cei, Salerno, Larcher, Salonia

Analysis and interpretation: Del Fabbro, Cicinelli, Lattanzio, Antropoli, Bianco, Larcher, Salonia, Bandello, Parodi

Obtained funding: N/A

Overall responsibility: Del Fabbro, Cicinelli, Bandello, Parodi

Abbreviations and Acronyms:
BCVA = best-corrected visual acuity; **CI** = confidence interval; **FA** = fluorescein angiography; **HR** = hazard ratio; **IRR** = incidence rate ratio; **IRF** = intraretinal fluid; **logMAR** = logarithm of the minimum angle of resolution; **PPV** = pars plana vitrectomy; **RD** = retinal detachment; **RH** = retinal hemangioblastoma; **UWF** = ultra-widefield; **VA** = visual acuity; **VHL** = von Hippel−Lindau.

Keywords:
Cumulative incidence, Retinal hemangioblastoma, Risk factors, Ultra-widefield imaging, Von, Hippel−Lindau.

Correspondence:
Sebastiano Del Fabbro MD, IRCCS San Raffaele Scientific Institute, Department of Ophthalmology, Via Olgettina, 60, Milan, Lombardy 20132, Italy. E-mail: delfabbro.sebastiano@hsr.it.

References

1. Maher ER, Iselius L, Yates JR, et al. Von Hippel-Lindau disease: a genetic study. *J Med Genet*. 1991;28:443−447.
2. Latif F, Tory K, Gnarra J, et al. Identification of the von Hippel-Lindau Disease tumor suppressor gene. *Science (1979)*. 1993;260:1317−1320.
3. Kaelin WG. Molecular basis of the VHL hereditary cancer syndrome. *Nat Rev Cancer*. 2002;2:673−682.
4. Maher ER, Neumann HP, Richard S. von Hippel−Lindau disease: a clinical and scientific review. *Eur J Hum Genet*. 2011;19:617−623.
5. Wong WT, Agrón E, Coleman HR, et al. Clinical characterization of retinal capillary hemangioblastomas in a large population of patients with von Hippel−Lindau disease. *Ophthalmology*. 2008;115:181−188.
6. Singh AD, Shields CL, Shields JA. von Hippel−Lindau disease. *Surv Ophthalmol*. 2001;46:117−142.
7. Toy BC, Agrón E, Nigam D, et al. Longitudinal analysis of retinal hemangioblastomatosis and visual function in ocular von Hippel-Lindau disease. *Ophthalmology*. 2012;119:2622−2630.
8. Daniels AB, Chang EY, Chew EY, et al. Consensus guidelines for ocular surveillance of von Hippel-Lindau disease. *Ophthalmology*. 2024;131:622−633.
9. Chen X, Sanfilippo CJ, Nagiel A, et al. Early detection of retinal hemangioblastomas in von Hippel-Lindau disease using ultra-widefield fluorescein angiography. *Retina*. 2018;38:748−754.
10. Wiley HE, Krivosic V, Gaudric A, et al. Management of retinal hemangioblastoma in von Hippel-Lindau disease. *Retina*. 2019;39:2254−2263.
11. World Health Organization (WHO). *Blindness and vision impairment*; 2022. https://icd.who.int/browse/2025-01/mms/en#1103667651. Accessed January 3, 2025.
12. Larcher A, Rowe I, Belladelli F, et al. Von Hippel−Lindau disease-associated renal cell carcinoma: a call to action. *Curr Opin Urol*. 2022;32:31−39.
13. Larcher A, Belladelli F, Cei F, et al. Centralization of care for rare genetic syndromes associated with cancer: improving outcomes and advancing research on VHL disease. *Nat Rev Urol*. 2024;21:565−571.
14. Louise M, Binderup M, Smerdel M, et al. von Hippel-Lindau disease: updated guideline for diagnosis and surveillance. *Eur J Med Genet*. 2022;65:104538.
15. Moussa G, Bassilious K, Mathews N. A novel excel sheet conversion tool from Snellen fraction to logMAR including 'counting fingers', 'hand movement', 'light perception' and 'no light perception' and focused review of literature of low visual acuity reference values. *Acta Ophthalmol*. 2021;99:e963−e965.
16. Krivosic V, Kamami-Levy C, Jacob J, et al. Laser-pPhotocoagulation for peripheral retinal capillary hemangioblastoma in von Hippel-Lindau disease. *Ophthalmol Retina*. 2017;1:59−67.
17. Krzystolik K, Stopa M, Kuprjanowicz L, et al. Pars plana vitrectomy in advanced cases of von Hippel-Lindau disease. *Retina*. 2016;36:325−334.
18. Silva PS, Cavallerano JD, Haddad NMN, et al. Peripheral lesions identified on ultrawide field imaging predict increased risk of diabetic retinopathy progression over 4 years. *Ophthalmology*. 2015;122:949−956.
19. Deák GG, Pulido JS, Jampol LM. Segmental diffuse vascular leakage: a fluorescein angiographic finding with von Hippel-Lindau disease. *Retin Cases Brief Rep*. 2021;15:628−631.
20. Richards S, Aziz N, Bale S, et al. Standards and guidelines for the interpretation of sequence variants: a joint consensus recommendation of the American College of medical genetics

and genomics and the association for molecular pathology. *Genet Med*. 2015;17:405−424.
21. Wiley HE, Srinivasan R, Maranchie JK, et al. Oral hypoxia-inducible factor 2α inhibitor Belzutifan in icular von Hippel-Lindau disease. *Ophthalmology*. 2024;131:1324−1332.
22. Larcher A, Belladelli F, Cei F, et al. Removing barriers to the use of systemic agents for patients with von Hippel-Lindau disease. *Eur Urol Oncol*. 2024;7:1141−1143.
23. Jonasch E, Donskov F, Iliopoulos O, et al. Belzutifan for renal cell carcinoma in von Hippel−Lindau disease. *New Engl J Med*. 2021;385:2036−2046.
24. Dollfus H, Massin P, Taupin P, et al. Retinal hemangioblastoma in von Hippel-Lindau disease: a clinical and molecular study. *Invest Ophthalmol Vis Sci*. 2002;43:3067−3074.
25. Kreusel K-M, Bechrakis NE, Krause L, et al. Retinal angiomatosis in von Hippel−Lindau disease. *Ophthalmology*. 2006;113:1418−1424.
26. Wang H, Shepard MJ, Zhang C, et al. Deletion of the von Hippel-Lindau gene in hemangioblasts causes hemangioblastoma-like lesions in murine retina. *Cancer Res*. 2018;78:1266−1274.
27. van Rooijen E, Voest EE, Logister I, et al. von Hippel-Lindau tumor suppressor mutants faithfully model pathological hypoxia-driven angiogenesis and vascular retinopathies in zebrafish. *Dis Model Mech*. 2010;3:343−353.
28. Knudson AG. Hereditary cancer: two hits revisited. *J Cancer Res Clin Oncol*. 1996;122:135−140.
29. Binderup MLM, Budtz-Jørgensen E, Bisgaard ML. Risk of new tumors in von Hippel−Lindau patients depends on age and genotype. *Genet Med*. 2016;18:89−97.
30. Pulido JS, Dalvin LA, Olsen TW, et al. Peripheral retinal nonperfusion using widefield imaging with von Hippel-Lindau disease. *Int J Retina Vitreous*. 2018;4:36.
31. Jampol LM, Goldbaum MH. Peripheral proliferative retinopathies. *Surv Ophthalmol*. 1980;25:1−14.
32. Nicholson L, Vazquez-Alfageme C, Patrao NV, et al. Retinal nonperfusion in the posterior pole is associated with increased risk of neovascularization in central retinal vein occlusion. *Am J Ophthalmol*. 2017;182:118−125.
33. Jansson RW, Frøystein T, Krohn J. Topographical distribution of retinal and optic disc neovascularization in early stages of proliferative diabetic retinopathy. *Invest Opthalmology Vis Sci*. 2012;53:8246.
34. Chan CC, Vortmeyer AO, Chew EY, et al. VHL gene deletion and enhanced VEGF gene expression detected in the stromal cells of retinal angioma. *Arch Ophthalmol*. 1999;117:625−630.